

Supporting Information

Enhancing Stable and High-Rate Lithium Ion Storage Through Multifunctional Molecular Release in Phosphorus/Carbon-Bipyridine Hybrid Anode

*Gengchang Lai^{a, b, †}, Zhilin Huo^{a, c, †}, Haoyu Wang^{a, d, †}, Zihui Liu^{a, d}, Zunbin Duan^{a, e}, Xiaoxiao Feng^a, Xiaoyi Zhang^a, Xin Fan^c, Xingchen He^{a, b, *}, Xue-Feng Yu^{a, b}, Jiahong Wang^{a, b, f, *}*

^a Shenzhen Institutes of Advanced Technology, Chinese Academy of Sciences, Shenzhen 518055, P. R. China.

^b University of Chinese Academy of Sciences, Beijing 100049, P. R. China.

^c College of Materials Science and Engineering, Guilin University of Technology, Guilin 541004, P. R. China.

^d Southern University of Science and Technology, Shenzhen 518055, P. R. China.

^e National Engineering Research Center for Colloidal Materials and School of Chemistry and Chemical Engineering, Shandong University, Jinan 250100, P. R. China.

^f Shenzhen University of Advanced Technology, Shenzhen, 518055 P. R. China.

[†] These authors contributed equally: Gengchang Lai, Zhilin Huo, Haoyu Wang.

* Corresponding authors: jh.wang1@siat.ac.cn (J. H. Wang); xc.he@siat.ac.cn (X. C. He)

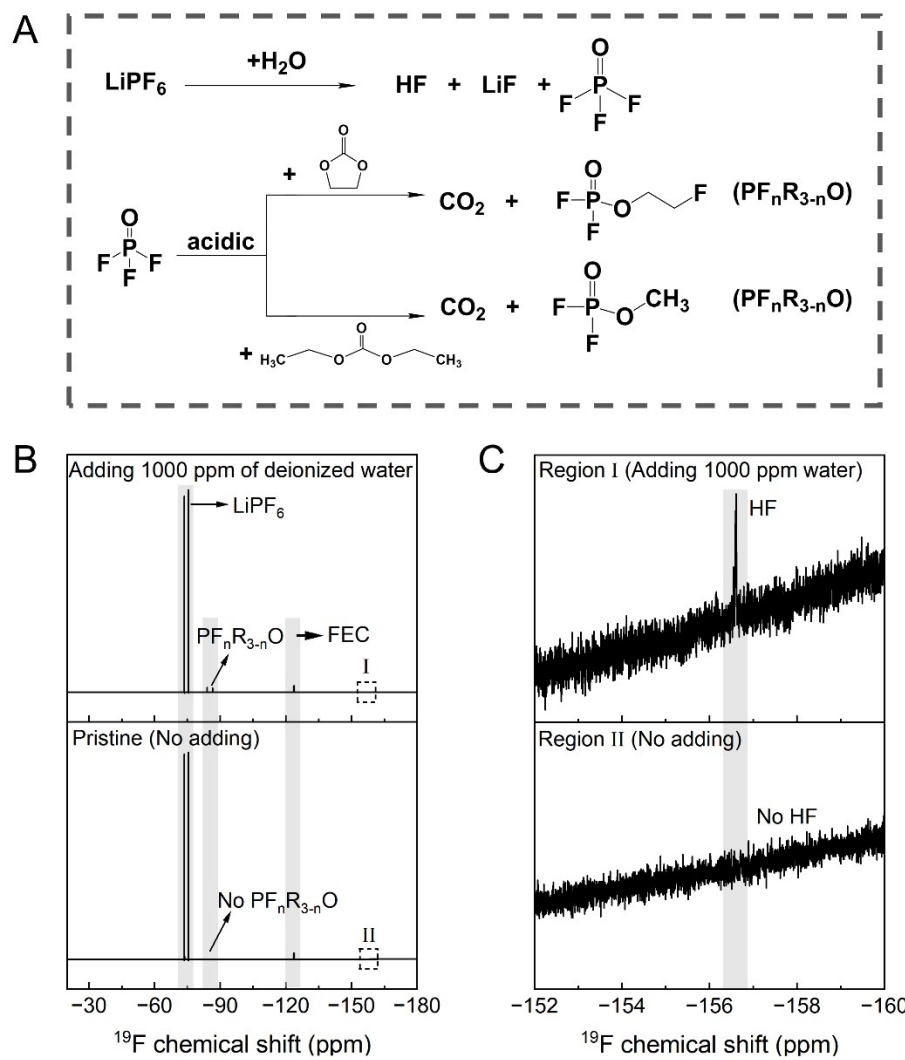


Figure S1. (A) Degradation mechanisms for LiPF_6 -based electrolytes (EC and DEC as co-solvents).¹⁻³ (B) ^{19}F NMR spectra of the 1 M LiPF_6 in EC-DEC-FEC-VC (47:47:5:1 in vol:vol:vol:vol; dodochem) electrolyte at the pristine stage (without adding deionized water) and after adding 1000 ppm of deionized water and leaving it for 24 hours. (C) An enlarged view of the $-152 \sim -160$ ppm region in panel (B).

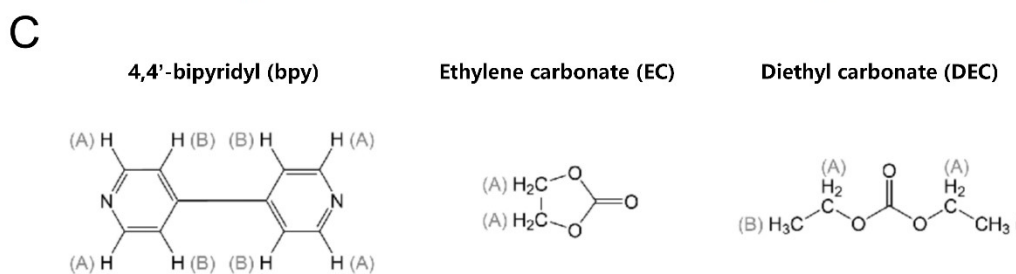
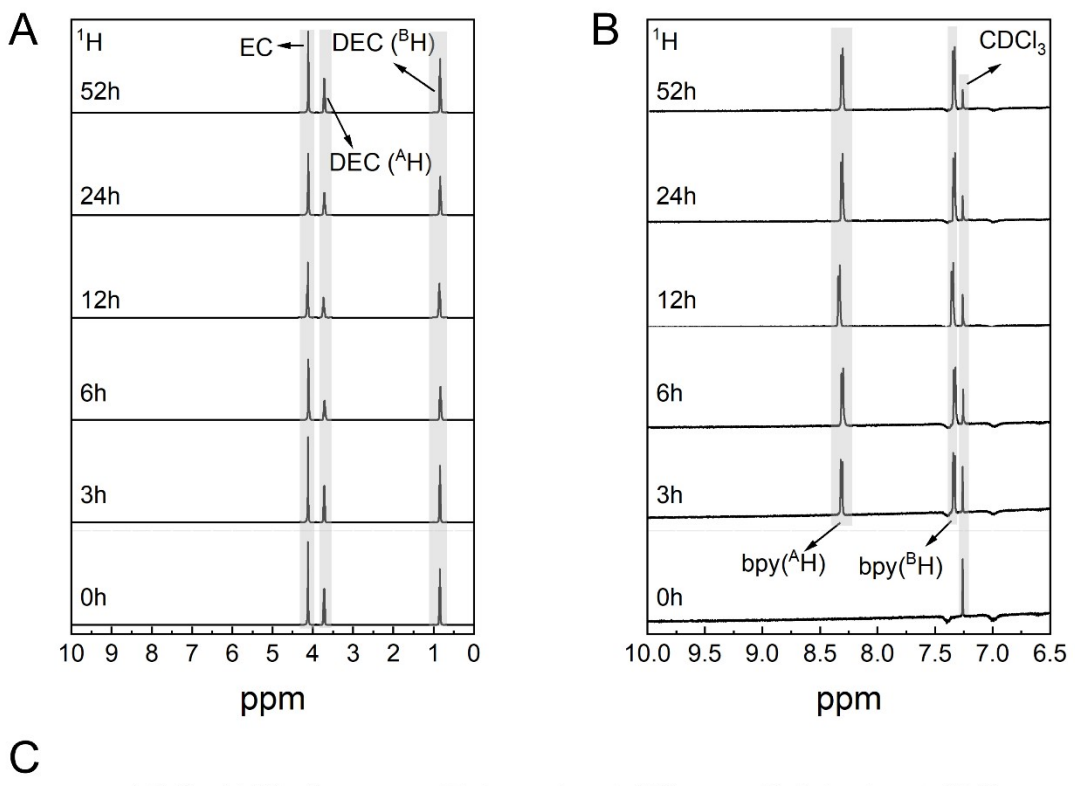


Figure S2. (A) ¹H NMR spectra of P/C-bpy sustained release solution after 0, 3, 6, 12, 24, and 52 h. (B) An enlarged view of the 6.5-10 ppm region in panel (A), which was calibrated using CDCl₃ (7.26 ppm) as the reference, and the ratio was calculated based on the peak values of bpy and CDCl₃ to reflect the sustained release concentration of bpy. (C) The different chemical environments of ¹H for 4,4'-bpy, EC, and DEC molecules.

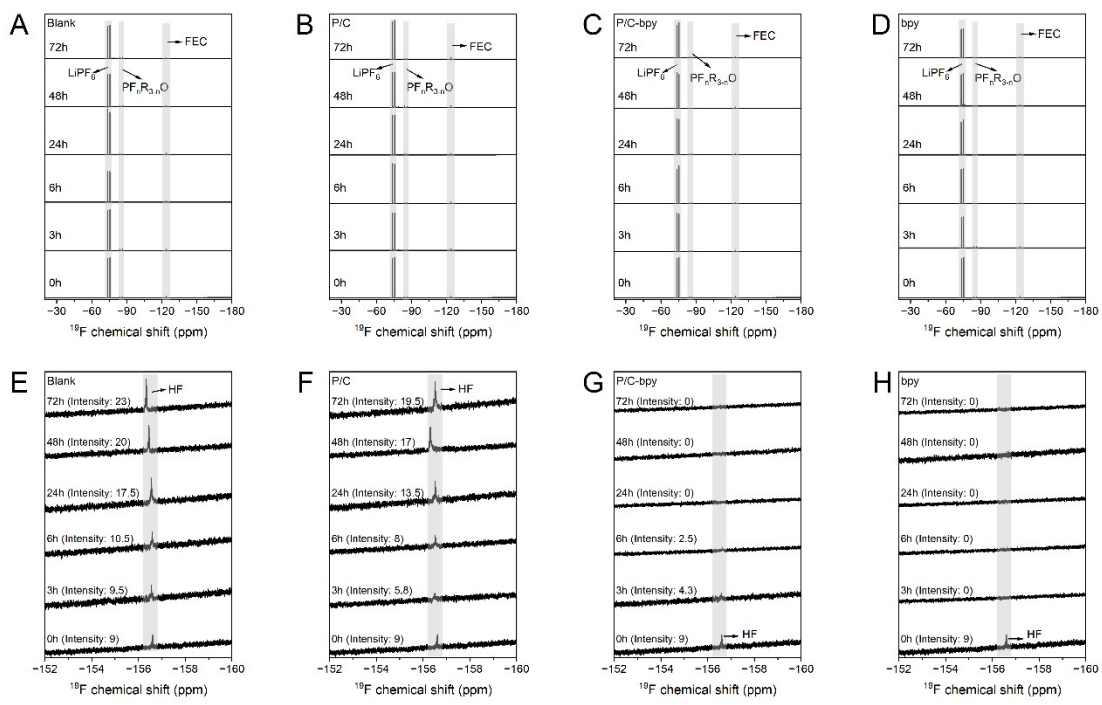


Figure S3. ^{19}F NMR spectra of the electrolyte at time intervals of 0, 3, 6, 24, 48, and 72 hours for (A) blank samples (without any additive), and containing (B) P/C, (C) P/C-bpy, (D) bpy. (E-H) An enlarged view of the -152 ~ -160 ppm region in panel (A-D).

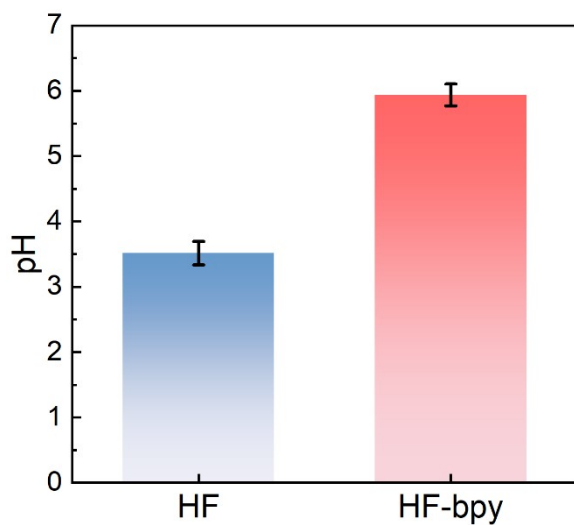


Figure S4. pH values of HF solution with or without bipyridine.

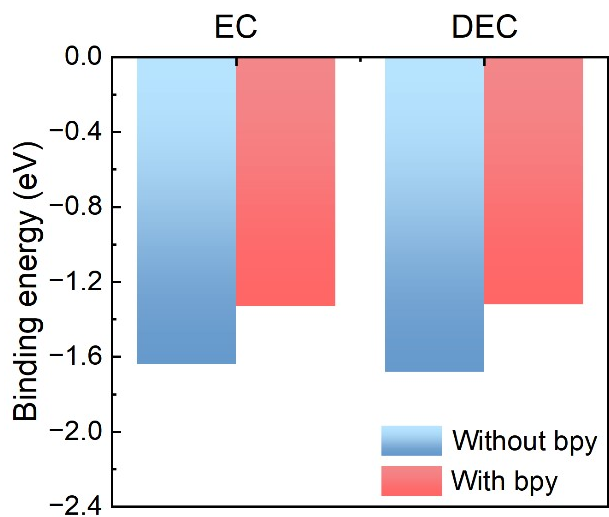


Figure S5. Binding energies of EC and DEC solvent molecules for lithium ions in the presence and absence of bpy.

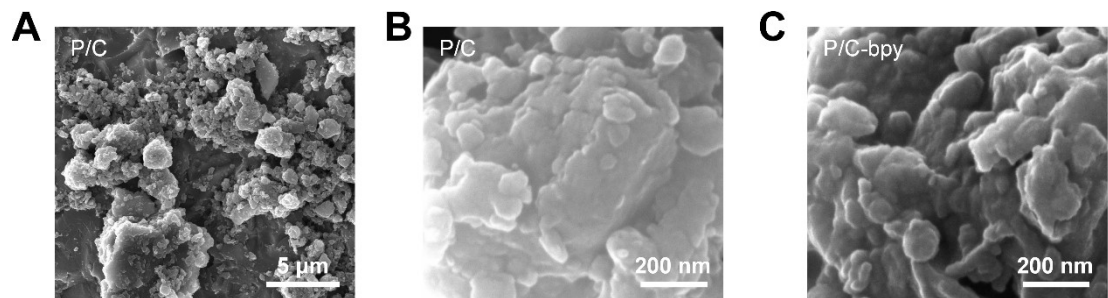


Figure S6. (A) and (B) SEM image of P/C at different magnifications. (C) SEM image of P/C-bpy.

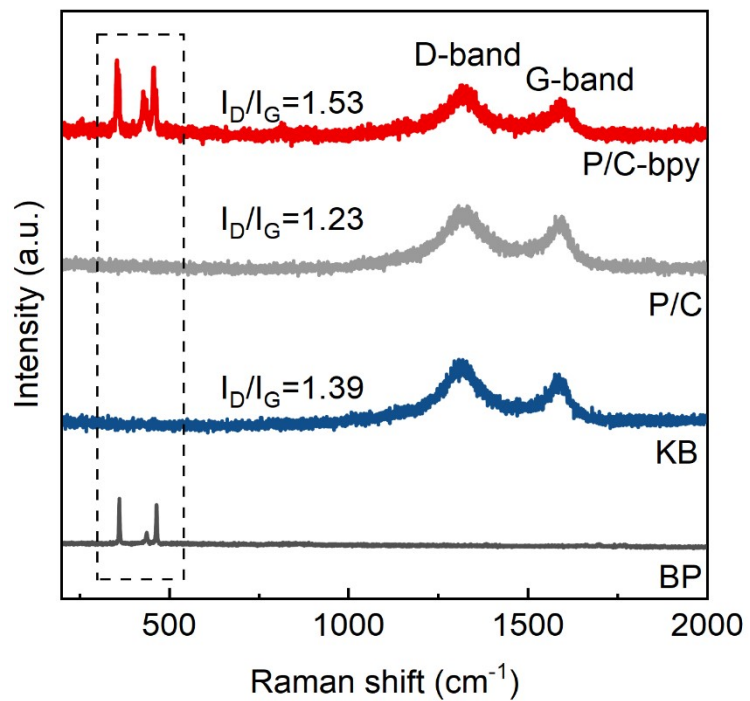


Figure S7. Raman scattering spectra of BP, KB, P/C, and P/C-bpy.

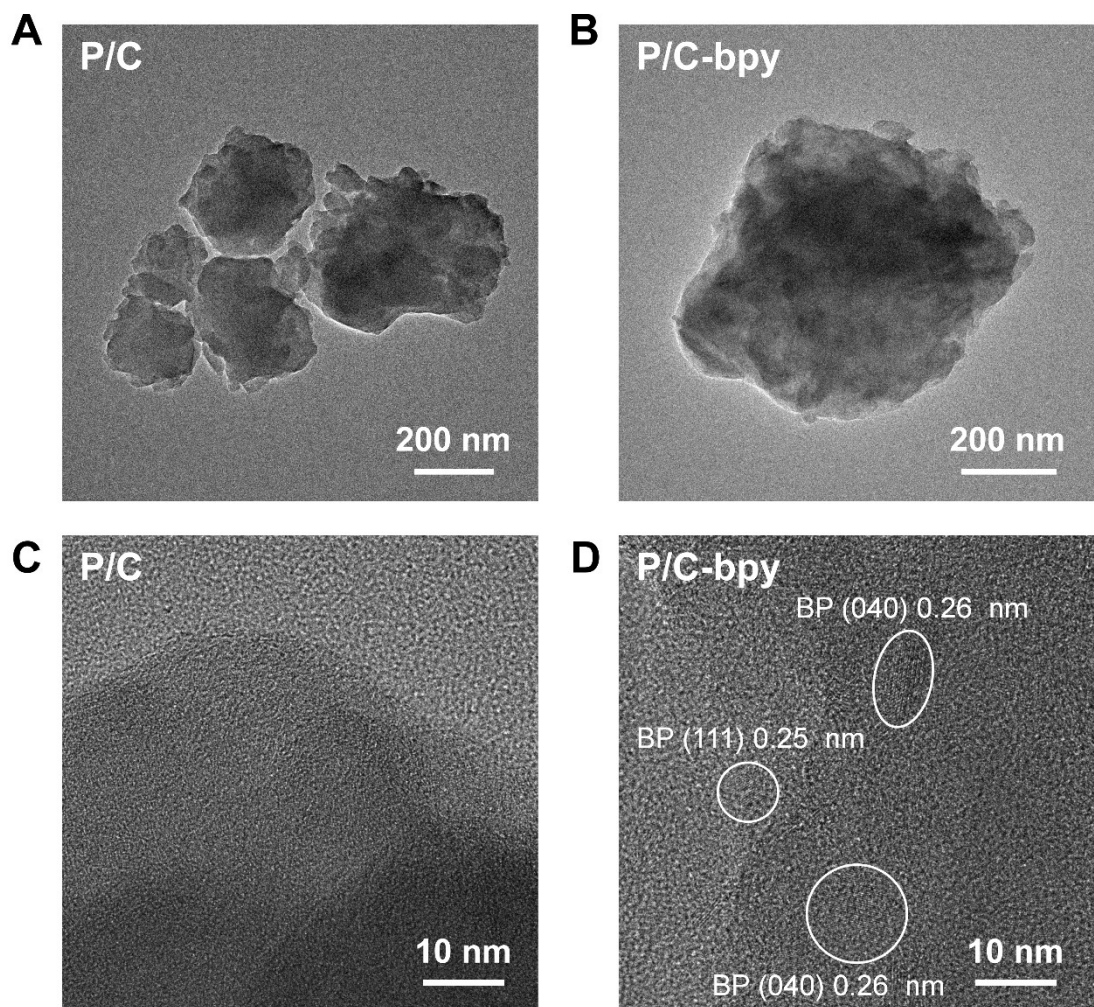


Figure S8. (A) and (C) TEM image of P/C at different magnifications. (B) and (D) TEM image of P/C-bpy at different magnifications.

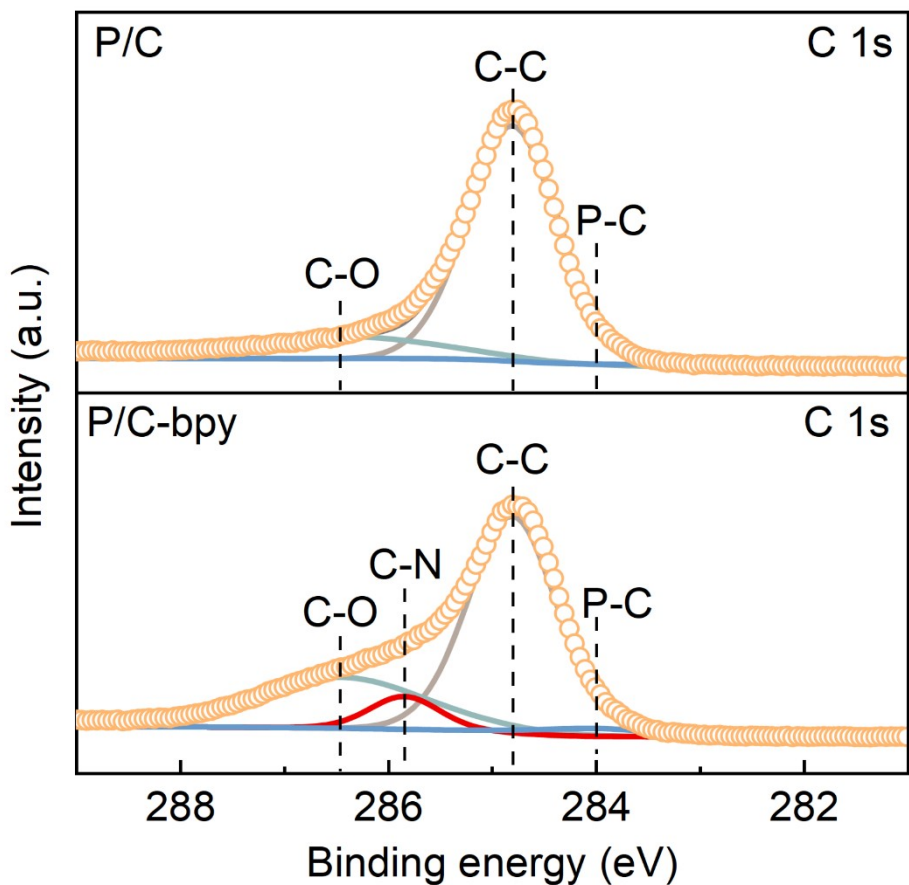


Figure S9. High-resolution C 1s XPS spectra of P/C and P/C-bpy.

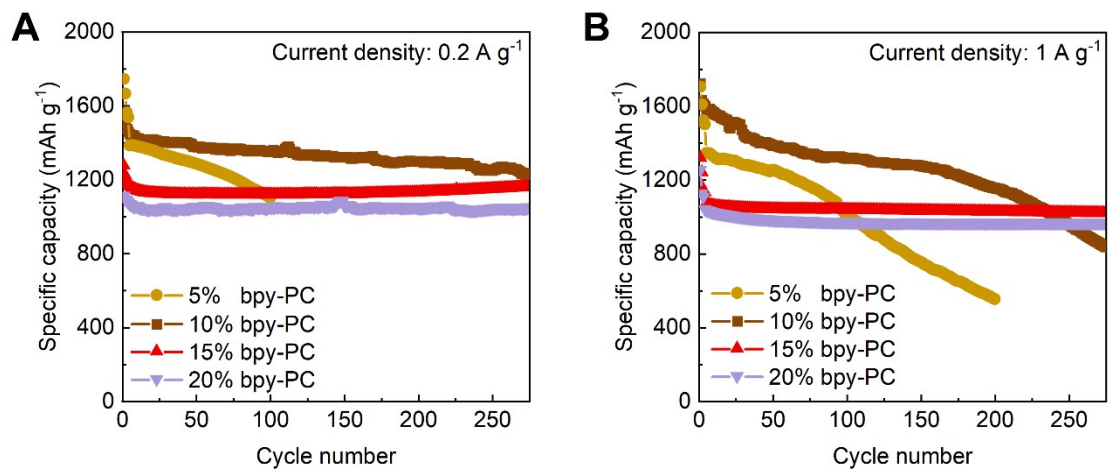


Figure S10. Cycling stability of different bipyridine-doped P/C materials of 5%, 10%, 15%, and 20% at current densities of (A) 0.2 and (B) 1.0 A g⁻¹.

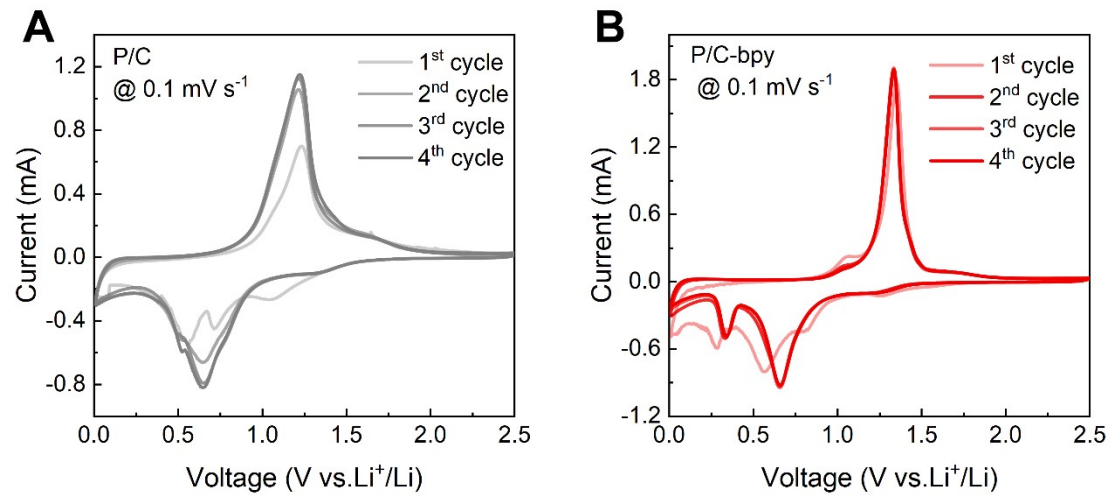


Figure S11. CV profiles of (A) P/C and (B) P/C-bpy at first 4 cycles of 0.1 mV s⁻¹.

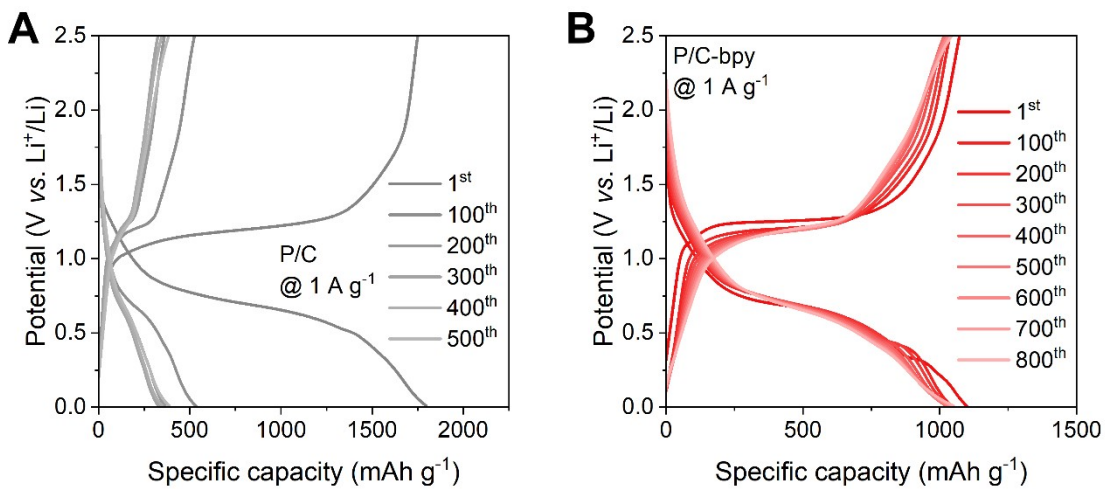


Figure S12. GCD curves of (A) P/C and (B) P/C-bpy at 1 A g⁻¹.

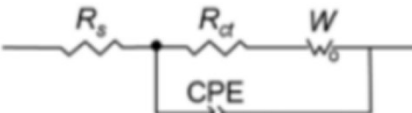
Pristine			
System	R_s (ohm)	R_{ct} (ohm)	k_w
P/C	2.169	397.3	1.4
P/C-bpy	5.235	286.1	3.2

Figure S13. Fitting circuit diagram based on the Nyquist of P/C and P/C-bpy before cycling and the corresponding solution resistance (R_s), charge transfer resistance (R_{ct}), and solid-phase diffusion factor (k_w : defined as the slope of the $-Z''$ vs. Z' curve at low frequency).

Cycled

The circuit diagram shows a series connection of five components: a resistor R_s , a CPE1 element, a resistor R_{int} , a CPE2 element, and a resistor R_{ct} . The CPE elements are represented by parallel lines with arrows pointing right. The circuit is completed by a Warburg impedance W connected to ground.

System	R_s (ohm)	R_{int} (ohm)	R_{ct} (ohm)	k_w
P/C	3.242	12.21	58.07	1.67
P/C-bpy	4.152	11.71	21.99	2.63

Figure S14. Fitting circuit diagram based on the Nyquist of P/C and P/C-bpy after cycling and the corresponding R_s , interface resistance (R_{int}), R_{ct} , and k_w .

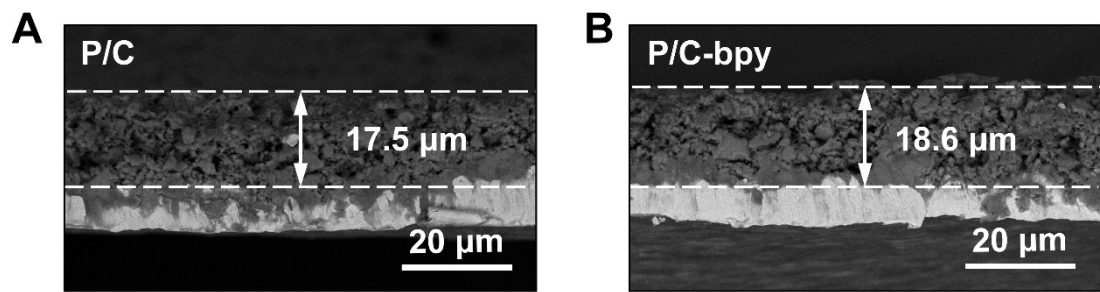


Figure S15. SEM image of the cross-section of the (A) P/C and (B) P/C-bpy electrode before cycling.

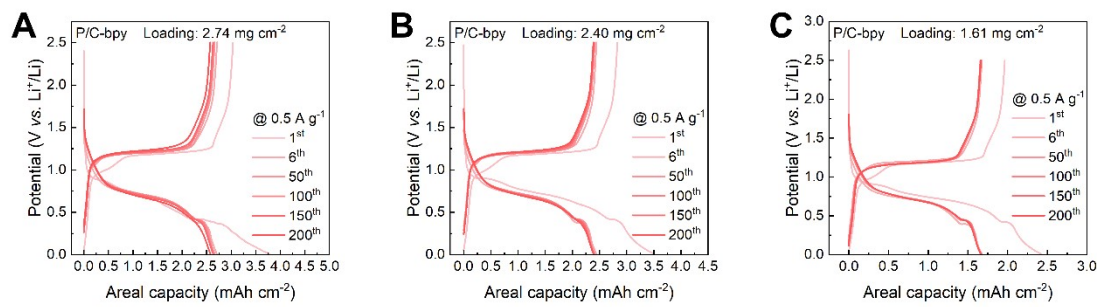


Figure S16. GCD curves of P/C-bpy at (A) 2.74 mg cm⁻², (B) 2.40 mg cm⁻², (C) 1.61 mg cm⁻² load under the current density of 0.5 A g⁻¹.

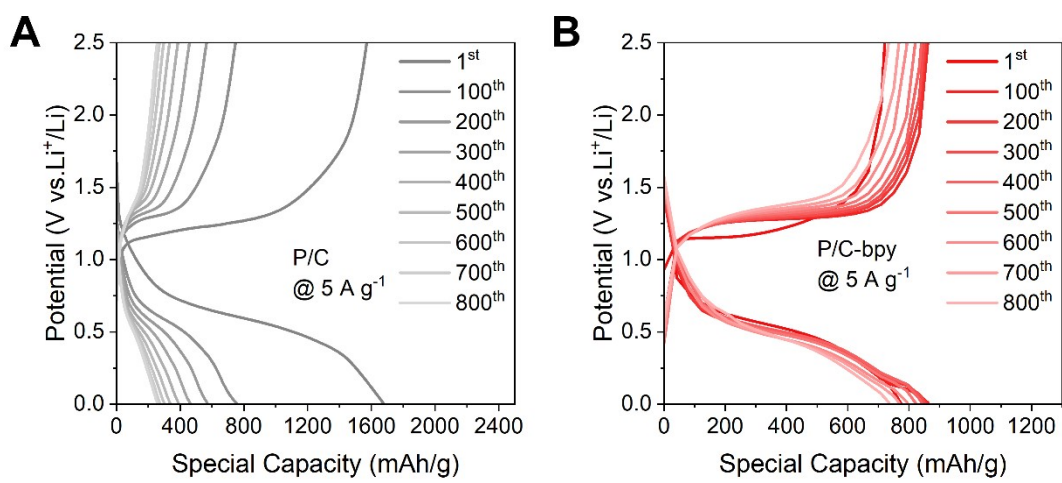


Figure S17. GCD curves of (A) P/C and (B) P/C-bpy at 5 A g⁻¹.

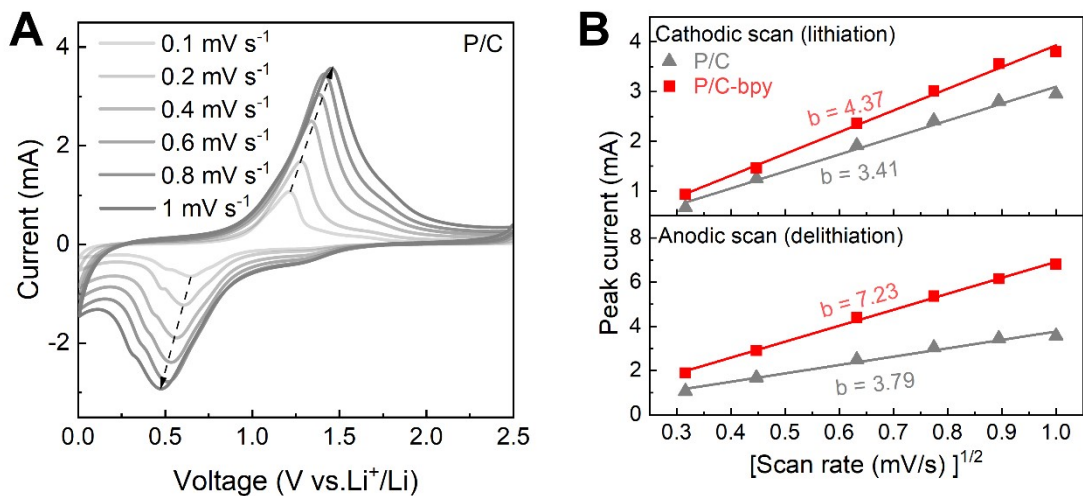


Figure S18. (A) CV curves of P/C at 0.1-1.0 mV s⁻¹ scan rates. (B) Lithium ion diffusion coefficients (D_{Li^+}) calculated from peak current and $(\text{scan rate})^{1/2}$ based on CV curves.

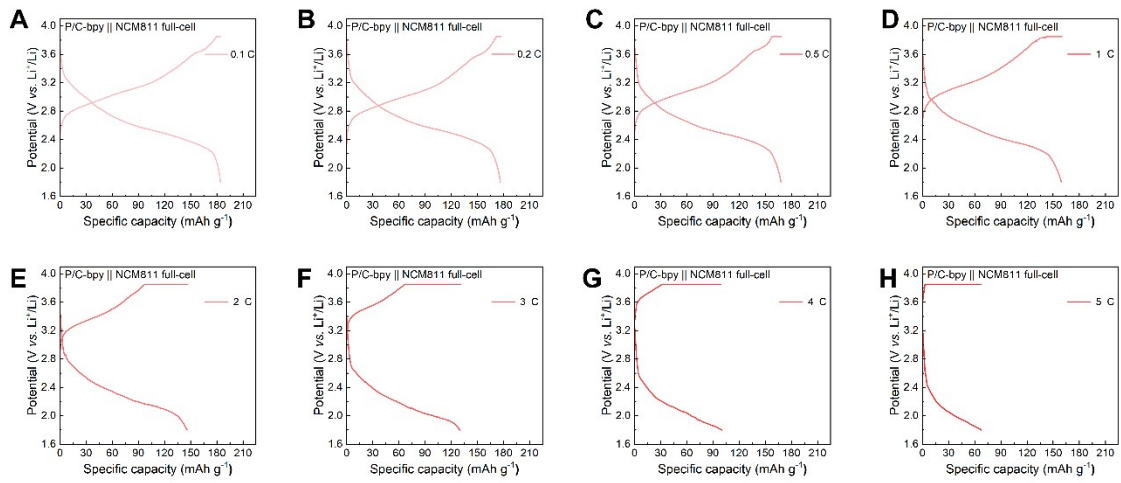


Figure S19. GCD curve of P/C-bpy || NCM811 full-cell at different current densities of (A) 0.1C, (B) 0.2C, (C) 0.5C, (D) 1C, (E) 2C, (F) 3C, (G) 4C, and (H) 5C.

Table S1. Comparison of cycle stability of P/C-bpy with reported phosphorus carbon materials.

Materials	Areal loading (mg cm ⁻²)	Current density (A g ⁻¹)	Cycle number	Capacity (mAh g ⁻¹)	Capacity retention	Refs.
P/C-bpy	0.7	1	800	1043.44	92.10%	This Work
	0.7	5	800	733.52	70.17%	
	1.61	0.5	200	1037.67	99.46%	
	2.40	0.5	200	996.58	97.84%	
	2.74	0.5	200	940.21	95.01%	
TpEB-FSI@P/G	-	0.89	500	1115	87.0%	[4]
		3.57	600	587	64%	
Sb@BP/C	1.2	0.2	100	719	70%	[5]
BP-GDYO	1.5-2.0	0.1	100	961	69%	[6]
		2	800	600	72%	
GDY/BP/GDY	0.2	0.1	200	902.3	88%	[7]
		10	800	424	70%	
HPPR	0.5	0.5	500	1201.4	81.90%	[8]
BP/G/CNTs	0.8-1.2	1	800	860	73%	[9]
		2	800	740	80%	
P/CNT@PI	-	1	500	450	56%	[10]
(BP-G)/PANI	1.2	2.6	800	950	85%	[11]
		5.2	800	790	93%	
		13	800	500	79%	
RP-PC	-	1	800	985	88.50	[12]
		8.32	800	516	70.98	
pMA-PC	0.7–0.8	0.2	100	1602	97.80%	[13]
		1	500	1120	86.70%	
		3	250	1040	82%	

Table S2 Comparison of rate performance of P/C-bpy with reported phosphorus carbon materials for LIBs.

Materials	Areal loading (mg cm ⁻²)	Current density (A g ⁻¹)	Capacity (mAh g ⁻¹)	Refs.
P/C-bpy	0.7	0.2	1318.20	
		0.5	1179.43	
		1	1091.42	
		3	942.15	This Work
		5	853.61	
		10	717.73	
TpEB-FSI@P/G	-	15	599.09	
		0.4	1238.8	
		0.9	1166.8	
		1.8	1087.9	[4]
		3.6	987.6	
		7.1	842.8	
Sb@BP/C	1.2	0.2	988	
		0.5	802	
		1	667	[5]
		2	568	
		5	451	
BP-GDYO	1.5-2.0	0.2	1276	
		0.5	955.9	
		1	795.2	[6]
		2	642.5	
		5	428.4	
GDY/BP/GDY	0.2	0.2	1331	
		0.5	1269	
		1	1087	
		2	906	[7]
		5	638	
HPRP	0.5	10	431	
		0.2	1474.7	
		0.5	1332.8	
		1	1173.3	[8]
		2	947.2	
BP/G/CNTs	0.8-1.2	5	532	
		0.3	1185.6	
		0.5	1119.5	
		1	1049.1	[9]
		2	985.8	
		3	914.9	

P/CNT@PI	-	0.25	1114.2	[10]
		0.5	1063.2	
		1	1017.6	
		2	969.6	
		4	904.4	
		6	843.3	
		8	771.1	
		10	705.5	
		2.6	1000	
(BP-G)/PANI	1.2	5.2	825	[11]
		13	575	
RP-PC	0.8–1.1 mg	0.26	1320.2	[12]
		1.04	1137.8	
		2.08	1069	
		4.16	971.2	
		6.24	813.8	
		8.32	649.5	

Notes: All the data are based on the active composite.

Table S3 Comparison of the cycling stability of the P/C-bpy || NCM811 full-cell with reported P-based full-cell.

Anode	Cathode	N:P	Loading (mg cm ⁻²)	Current density (C)	Cycle number	Specific capacity (mAh g ⁻¹)	Capacity retention	Refs.
P/C-bpy	NCM811	1.1	10.2	1	900	124.3	80.9%	This Work
Prelihiated P/C	LCO	1.1	3.0-4.0	1	900	104	91.2%	[14]
f-P	LCO	1.1	13.3	1	200	118	92.8%	[15]
Red-P/VAG	LCO	1.1–1.2	28.0–28.4	6	450	92.2	70%	[16]
P/C	LNMO	1.1	-	0.3	200	97.5	97%	[17]
RP@P-PC	LFP	1.1-1.5	7.0-9.0	2.9	100	132	80.0%	[18]
FP-G	LFP	1.1	-	0.65	200	114.2	83%	[19]
FP-G	NCM532	1.1	-	0.65	150	103	74.6%	[19]
RPNPs	NCM532	1.1	3.08	1.48	120	74.7	75.0%	[20]
BP/KB-MWCNTs	NCM622	1.1	9.0	0.2	100	161.1	88.0%	[21]
Red-P/VAG	NCM622	1.1–1.2	26.6–29.0	4 6	350 350	77.3 66.9	80.6% 76.9%	[16]
BP-Mo-CNT	NCM811	1.1	10.1	1	300	148.6	84.6%	[22]
P@ZTC	NCM811	1.2	4.8 5.4	0.1 0.5	100 900	124 80	76.1% 70.8%	[23]
RP	NCM811	1.1	11.61	0.5 1	200 200	118 107	74% 69%	[24]

Notes: The loading, current density and specific capacity were calculated based on the active material of the cathode.

Table S4 Comparison of rate performance of the P/C-bpy || NCM811 full-cell with reported P-based full-cell.

Anode	Cathode	N:P	Loading (mg cm ⁻²)	Current density (C)	Specific capacity (mAh g ⁻¹)	Refs.
P/C-bpy	NCM811	1.1	10.2	0.1	182.82	
				0.2	176.55	
				0.5	168.33	
				1	160.25	This
				2	147.83	Work
				3	130.39	
RP/C	LCO	1.1	-	4	98.78	
				5	67.92	
				0.2	167	
				0.5	158	
f-P	LCO	1.1	13.3	1	153	[25]
				2	144	
				0.2	139.1	
				0.5	132.3	
P/C	LNMO	1.1	-	1	122.6	[15]
				2	107.5	
				3	96.2	
				0.3	107	
BP@Cu Foam	LFP	1.1	5.5	0.5	98	
				1	84	[17]
				2	76	
				3	68	
Red-P/VAG	NCM622	1.1–1.2	26.6–29.0	0.2	162	
				0.5	160	
				1	153	[26]
				2	143	
BP/KB-MWCNTs	NCM622	1.1	9	0.2	194.24	
				1	176.26	
				2	154.68	[16]
				4	111.51	
BP-Mo-CNT	NCM811	1.1	10.1	6	93.53	
				0.2	182	
				0.4	176	
				0.6	170	[21]
				0.8	164	
				1	156	
				1.5	146	
				0.5	157.86	[22]

					1	146.66	
					2	136.68	
					3	126.07	
					4	109.55	
					5	100.5	
P@ZTC	NCM811	1.2	5.4	[23]	0.1	181	
					0.2	158	
					0.3	143	
					0.4	130	
					0.5	121	
					1	90	
					0.1	151.6	
RP	NCM811	1.1	11.61	[24]	0.2	140.1	
					0.3	126.2	
					0.4	113.4	
					0.5	109.4	
					1	83.40	
					2	50.20	

Notes: The loading, current density and specific capacity were calculated based on the active material of the cathode.

Reference:

1. L. Sheng, K. Yang, J. Chen, D. Zhu, L. Wang, J. Wang, Y. Tang, H. Xu and X. He, *Adv. Mater.*, 2023, **35**, 2212292.
2. L. Ding, Y. Chen, Y. Sheng, X. Yue and Z. Liang, *Angew. Chem., Int. Ed.*, 2024, **63**, e202411933.
3. S. Jiang, R. Li, L. Chen, C. Sun, J. Wang, J. Zheng, L. Chen, T. Deng and X. Fan, *Adv. Mater.*, 2025, **37**, 2417285.
4. Y. Cao, S. Zhang, B. Zhang, C. Han, Y. Zhang, X. Wang, S. Liu, H. Gong, X. Liu, S. Fang, F. Pan and J. Sun, *Adv. Mater.*, 2022, **35**, 2208514.
5. Y. Ma, K. Wang, Y. Xu, X. Zhang, Q. Peng, Y. Guo, X. Sun, X. Zhang, Z. S. Wu and Y. Ma, *Adv. Energy Mater.*, 2024, **14**, 2304408.
6. T. Wang, M. Li, L. Yao, W. Yang and Y. Li, *Adv. Mater.*, 2024, **36**, 2402961.
7. Q. Chang, X. Fu, J. Gao, Z. Zhang, X. Liu, C. Huang and Y. Li, *Adv. Mater.*, 2023, **35**, 2305317.
8. J. Zhu, Z. Liu, W. Wang, L. Yue, W. Li, H. Zhang, L. Zhao, H. Zheng, J. Wang and Y. Li, *ACS Nano*, 2021, **15**, 1880-1892.
9. M. Li, W. Li, Y. Hu, A. A. Yakovenko, Y. Ren, J. Luo, W. M. Holden, M. Shakouri, Q. Xiao, X. Gao, F. Zhao, J. Liang, R. Feng, R. Li, G. T. Seidler, F. Brandys, R. Divigalpitiya, T. K. Sham and X. Sun, *Adv. Mater.*, 2021, **33**, 2101259.
10. M. Han, S. Zhang, Y. Cao, C. Han, X. Li, Y. Zhang, Z. Yang and J. Sun, *J. Energy Chem.*, 2022, **70**, 276-282.
11. H. Jin, S. Xin, C. Chuang, W. Li, H. Wang, J. Zhu, H. Xie, T. Zhang, Y. Wan, Z. Qi, W. Yan, Y.-R. Lu, T.-S. Chan, X. Wu, J. B. Goodenough, H. Ji and X. Duan, *Science*, 2020, **370**, 192-197.
12. S. Zhang, C. Liu, H. Wang, H. Wang, J. Sun, Y. Zhang, X. Han, Y. Cao, S.

- Liu and J. Sun, *ACS Nano*, 2021, **15**, 3365-3375.
13. Z. Huo, Z. Duan, X. Feng, H. Wang, H. Huang, X. Fan, R. He, X. F. Yu and J. Wang, *Small*, 2024, **20**, 2402483, DOI: 10.1002/smll.202402483.
14. G. Wang, F. Li, D. Liu, D. Zheng, C. J. Abeggien, Y. Luo, X.-Q. Yang, T. Ding and D. Qu, *Energy Storage Mater.*, 2020, **24**, 147-152.
15. Z. Duan, X. Feng, G. Lai, D. Liu, X. Zhang, H. Wang, S. Chen, X. He, Z. Liu, L. Tong, H. Wang, X.-F. Yu and J. Wang, *J. Colloid Interface Sci.*, 2025, **679**, 161-170.
16. S. Tu, Z. Lu, M. Zheng, Z. Chen, X. Wang, Z. Cai, C. Chen, L. Wang, C. Li, Z. W. Seh, S. Zhang, J. Lu and Y. Sun, *Adv. Mater.*, 2022, **34**, 2202892.
17. J. Jiang, Y. Lin, H. You, M. Yao, J. Sun, L. Chen and C. Li, *Ind. Eng. Chem. Res.*, 2024, **63**, 13252-13260.
18. X. Han, X. Meng, S. Chen, J. Zhou, M. Wang, L. Sun, Y. Jia, X. Peng, H. Mai, G. Zhu, J. Li, C. W. Bielawski and J. Geng, *ACS Appl. Mater. Interfaces*, 2023, **15**, 11713-11722.
19. X. Gao, L. Liu, L. Zu, H. Lian, X. Cui and X. Wang, *J. Power Sources*, 2024, **595**, 234077.
20. W.-C. Chang, K.-W. Tseng and H.-Y. Tuan, *Nano Lett.*, 2017, **17**, 1240-1247.
21. R. Amine, A. Daali, X. Zhou, X. Liu, Y. Liu, Y. Ren, X. Zhang, L. Zhu, S. Al-Hallaj, Z. Chen, G.-L. Xu and K. Amine, *Nano Energy*, 2020, **74**, 104849.
22. S. Chen, G. Lai, X. Zhang, X. Feng, L. Tong, C. Peng, X. He, Y. Li and J. Wang, *ACS Appl. Nano Mater.*, 2024, **7**, 24663-24672.
23. S. Wang, D. Liu, Y. Chen, H. Gao, J. Li, H. Tang and D. Qu, *ACS Appl. Mater. Interfaces*, 2024, **16**, 38041-38052.
24. S. Fang, C. Han, S. Zhang, Y. Cao, K. Ma, Y. Zhang, X. Han, J. Wang and J.

- Sun, *Small*, 2024, **20**, 2401204.
25. M. Liu, E. Zhou, C. Wang, Y. Ye, X. Tong, Y. Xie, S. Zhou, R. Huang, X. Kong, H. Jin and H. Ji, *Small*, 2023, **19**, 2208282.
26. Y. Wang, H.-Q. Sang, W. Zhang, Y. Qi, R.-X. He, B. Chen, W. Sun, X.-Z. Zhao, D. Fu and Y. Liu, *ACS Appl. Mater. Interfaces*, 2020, **12**, 51563-51572.